



The effect of surfactants modification on nanocrystalline cellulose for paclitaxel loading and release study

Jindrayani Nyoo Putro^a, Suryadi Ismadji^{b,*}, Chintya Gunarto^a, Maria Yuliana^b, Shella Permatasari Santoso^b, Felycia Edi Soetaredjo^b, Yi Hsu Ju^{c,*}

^a Department of Chemical Engineering, National Taiwan University of Science and Technology, No. 43, Sec 4, Keelung Rd, 10607 Taipei, Taiwan

^b Department of Chemical Engineering, Widya Mandala Surabaya Catholic University, Kalijudan 37, Surabaya 60114, Indonesia

^c Graduate Institute of Applied Science and Technology, National Taiwan University of Science and Technology, No. 43, Sec 4, Keelung Rd, 10607, Taipei, Taiwan

ARTICLE INFO

Article history:

Received 29 January 2019

Received in revised form 4 March 2019

Accepted 7 March 2019

Available online 08 March 2019

Keywords:

Nanocrystalline cellulose

Surfactant

Paclitaxel

Drug delivery

ABSTRACT

The Nanocrystalline cellulose (NCC) was prepared from filter paper by acid hydrolysis process. The modification of NCC with cationic, anionic, and nonionic surfactant did not have a tremendous effect on the chemical structure of material based on the characterization of XRD and FTIR. The modified NCCs were employed as a drug carrier for paclitaxel (PTX). Increasing concentration of ionic surfactants can enhance the loading of the hydrophobic drug, while the opposite trend was observed for nonionic surfactant modified nanocrystals. The attachment of surfactant toward the particle was a more likely physical aggregation of micelle on the surface of nanocrystals. Larger particle size was observed after the modification of nanocrystalline cellulose. The fitting of Higuchi and sigmoidal models were applied in the release profile to investigate the kinetic release mechanism of paclitaxel at pH 5.8 and 7.4. Cell viability was determined to check the biocompatibility of the materials toward mouse osteoblast cells 7F2 using MTT assay. Toxic behavior was not observed for NCC, while CTAB was completely not compatible with cells.

© 2019 Elsevier B.V. All rights reserved.

1. Introduction

Cellulose has been widely known as a versatile material for many industries, due to its ubiquity, cheap, and non-toxic properties. It has gained interests as a drug excipient in drug delivery systems, especially for the hydrophobic drugs loading [1–4]. Paclitaxel is one of the most potent tubulin inhibitors which can induce mitotic arrest of the cells life cycle. However, it has poor solubility in water and low availability [5,6]. The commercial paclitaxel was sold with the composition of Cremophor EL, which has an adverse side effect toward patients such as hypersensitivity reactions and neurotoxicity [7–9]. Nanotechnologies have given huge impact in drug delivery system in the last decades since it can overcome the low solubility and availability of drugs [10]. The formulation of nanoparticles in drug delivery can help therapeutics agent to get through the biological barriers, enhance the drug delivery, and reduce any toxicity from free drug toward normal cells [11,12]. Nanocrystalline cellulose (NCC) has a very small diameter with the range length of 100–250 nm; it has promising activity as a drug carrier due to its biocompatibility and large surface area [3]. The most common method to prepare NCC is sulfuric acid hydrolysis, which is very simple and gives

negative surface charge due to the grafting of sulfonate ion on the hydroxyl group surface. Because polysaccharide has hydrophilic nature, modification of surface is needed to alter the hydrophilicity of NCC for the adsorption of paclitaxel. Recent studies also revealed that NCC could be a good candidate as a disintegrant for oral drug delivery with the combination of calcium carbonate, which can increase the disintegration time dependent on the ratio and tableting time [13]. The combination of NCC with PEG and glycerol as capsule ingredient also has a similar release percentage with the gelatin-based capsule material, which can be an alternative in the pharmaceutical industry to avoid the harmful and toxic treatment of gelatin [14].

The surfactant has an amphiphilic structure that consisted of the hydrophobic tail and a hydrophilic head. Based on its charge, there are four types of surfactant: cationic, anionic, zwitterionic, and nonionic. A distinct characteristic of surfactant is its micelle formulation in the aqueous solution which has a lot of advantages in drug delivery applications [15]. Several studies showed that the addition of surfactant could greatly enhance the adsorption of the lipophilic drug on polysaccharide based nanoparticles. The surface modification using surfactant is also beneficial in drug delivery systems, because of its antimicrobial and anti-tumor activity [1,16]. The nonionic surfactant is preferable to use in drug delivery since it has lower critical micelle concentration than an ionic surfactant. However, NCC has a negative charge due to the attachment of sulfate ester, hence the possibility of using cationic, anionic, and

* Corresponding authors.

E-mail addresses: suryadiismadji@yahoo.com (S. Ismadji), yhju@mail.ntust.edu.tw (Y.H. Ju).

nonionic is explored in this study. It was also suggested that material with negative charge could prevent unnecessary interaction in mononuclear phagocyte system which prolongs the drug life in the blood circulation [17,18].

2. Materials and methods

2.1. Chemicals

The filter paper was purchased from Advantech no. 5C, with a diameter of 90 mm and ash content of 0.08 mg per circle. H₂SO₄ (Scharlau: 95–98%), NaOH (Fisher Scientific: NF/FCC grade), HCl (Acros; 37%), NaCl and KCl (Showa Chemical Co., Ltd.: 99.5%), KH₂PO₄ and NH₂PO₄·H₂O (J.T.Baker: A.C.S. Reagent), Ethanol anhydrous (Echo: >99.5%) were used in this experiment. There are 3 surfactants used in this study: cetyltrimethylammonium bromide (CTAB, Alfa Aesar: 98%), Sodium dodecyl sulfate (SDS, Sigma Aldrich: ≥99%), and Tween 20 (Wako Pure Chemical Industries, Ltd.). All of the chemicals were directly used without further purification.

2.2. Preparation and modification of NCC

The filter paper was shredded using a commercial blender and dried in the oven to remove excess moisture content. 1 g of shredded filter paper was hydrolyzed with 20 mL of 64 wt% H₂SO₄ for 60 min at 45 °C under mechanical stirring. The suspension was centrifuged (9503 ×g, 10 min) to separate the acid throughout the hydrolysis step, and subsequently put in dialysis tubing (MWCO: 10–14 kDa) against reversed osmosis water to remove the free acid in the NCC suspension. After the dialysate reached constant pH around 5, the suspension was put in an ultrasound bath for 30 min to make it well-dispersed and kept in –20 °C refrigerator for further lyophilization to obtain the dry NCC.

Dried NCC was modified with CTAB, SDS, and Tween 20. One hundred mg of NCC (0.25 wt% in suspension) was reacted with each surfactant at various concentration (5, 10, 15 mM) with and without the addition of 10 mM NaCl. NCC suspension was mixed at 200 rpm in 37 °C orbital shaker incubator for 24 h. Modified NCC was separated from the solution by centrifugation at 9503 ×g for 5 min, and kept in –20 °C for subsequent freeze drying.

2.3. Drug loading and release

Due to its poor solubility in water, paclitaxel (PTX) was dissolved using anhydrous ethanol with the concentration of 20, 40, 60, 80, and 100 µg/mL. 1 mL of drug solution was mixed with modified NCC (2 mg) in the microcentrifuge tube; the reaction was conducted for 30 min at 20 °C with 200 rpm shaker incubator. The PTX-modified NCC suspension was centrifuged at 9503 ×g for 5 min, to separate the unbound drug in the supernatant which was subsequently analyzed using UV–Vis spectrophotometer at 231 nm. PTX@modifiedNCC was freeze-dried and stored at a desiccant box for further use. The loading content (LC) and loading efficiency (LE) were calculated using the following equations:

$$\text{Loading content (LC, mg/g)} = \frac{(C_o - C_e)V}{m} \quad (1)$$

$$\text{Loading efficiency (LE, \%)} = \frac{(C_o - C_e)}{C_o} 100\% \quad (2)$$

where C_o and C_e (µg/mL) are initial and equilibrium drug concentration in the solution, respectively. V is the volume of the solution (mL) and m is the weight of modified NCC (mg).

For characterization using spectrophotometer, 3 mL of PTX solution was mixed with 7 mL of ethanol and pH 7.40 phosphate buffer saline

(PBS) (30:70, v/v). A calibration curve was prepared using linear regression in the determined concentration range with R² value of 0.9975.

In vitro drug release study of PTX@modifiedNCC was conducted by blood plasma environment. 2 mg of PTX@modifiedNCC immersed in 5 mL of pH 7.40 simulated body fluid (PBS 10 mM) and phosphate buffer pH 5.8 containing 30% vol. alcohol. The solution was placed in 100 mL closed Erlenmeyer flask, and put in an orbital shaker incubator at 37 °C with gentle agitation. At a certain time interval, 3 mL of solution was taken out, and 3 mL of fresh medium was added into the system. The sample was centrifuged before UV/Vis spectrophotometer at wavelength 231 nm. The release profile (%) was plotted using this equation:

$$\text{Release profile (\%)} = \frac{C_t}{C_o} 100\% \quad (3)$$

where C_t and C_o are the released and initial drug loaded concentration in the NCC, respectively. The release profile was plotted with respect to concentration versus time.

2.4. *In vitro* cell cytotoxicity

Mouse bone marrow (7F2) cells were cultured in HO-MEM medium supplemented with 10% (v/v) fetal bovine serum at 37 °C in 5% CO₂ environment for 24 h. Cells were seeded in 96-well plate with a density of 1 × 10⁴ cells/well, and incubated for 24 h. Cells proliferation was determined by MTT colorimetric assay [19]. NCC and modified NCC were sterilized under UV irradiation for one night in room temperature. Modified NCCs were put in FBS free HO-MEM with a concentration range of 10, 25, 50 and 100 µg/mL. The cells medium was replaced with nanoparticles suspension, incubated for 24 h. Then 20 µL of MTT (5 mg/mL in PBS) was added into each well and incubated for 4 h. Afterward, the MTT containing medium was removed and 200 µL DMSO was added to dissolve the formazan crystals. Absorbance value was measured using a microplate reader (BioTek PowerWave XS) at 570 nm. The cell viability was determined using the following equation:

$$\text{Cell viability (\%)} = \frac{\text{Absorbance with NPs}}{\text{Absorbance blank}} 100\% \quad (4)$$

2.5. Characterizations of un-/modified NCC

Surface morphology of each sample was characterized using a scanning electron microscope (FESEM-JEOL JSM-6500F). The samples were sputtered with a thin layer of platinum by a fine auto coater (JFC-1600, JEOL, Ltd., Japan) for 90 s in Ar atmosphere. Fourier transform infra-red (Shimadzu FTIR-8400S) was conducted in the wavenumber of 4000–500 cm⁻¹ with a scanning resolution of 4 cm⁻¹ and the signal was accumulated from 100 scans. The surface charge and particle size were analyzed using Zeta Potential PALS (Zeta Potential Analyzer, Brookhaven 90Plus), each of dried sample was dissolved in deionized water with a concentration of 0.01% wt. The zeta potential was calculated using the Smoluchowski equation built-in program, and particle size distribution was measured with a dynamic light scattering system. X-ray diffraction (XRD, Bruker D2 Phaser) were obtained using high monochromatic intensity Cu K_{α1} radiation (λ = 0.1541 nm) at 40 kV and 30 mA.

3. Results and discussions

3.1. Characterizations of un-/modified NCC

Morphology of nanomaterial was captured using SEM; Fig. 1A is the filter paper before acid hydrolysis. It can be seen that after going through sulfuric acid hydrolysis, NCC was formed rod-like crystals particles (Fig. 1B). During the modification with CTAB and SDS, the NCC

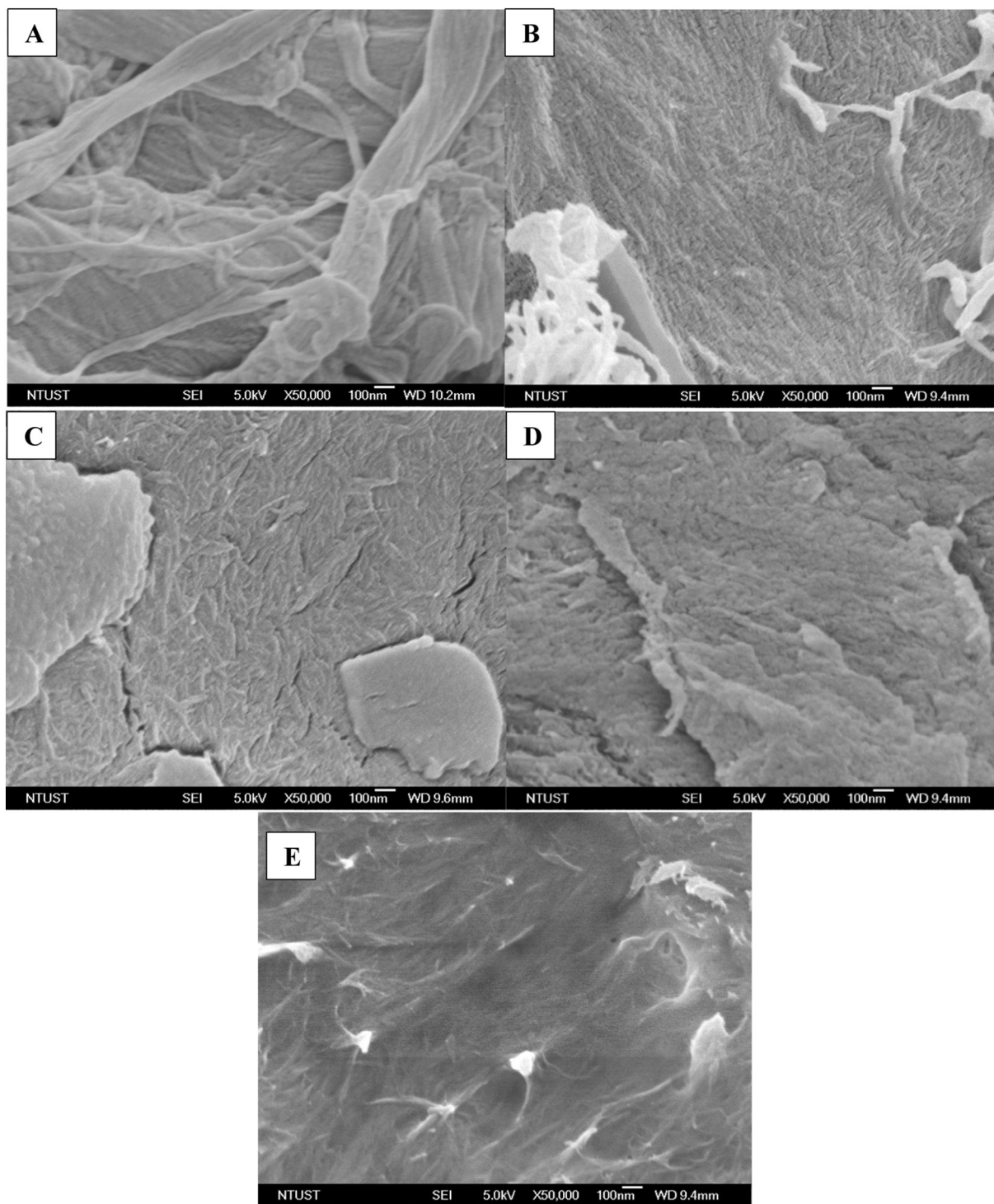


Fig. 1. Morphological images of (A) filter paper, (B) NCC, (C) CTAB-NCC, (D) SDS-NCC, (E) Tween 20-NCC.

particle has a denser surface morphology, and there is an obvious increase in the thickness of particle size. Nonionic surfactant, Tween 20 modified NCC resulted in longer rods than the other charged surfactant which has different morphologies than the ionic modified NCC. It can be seen in Fig. 1E, there is an entanglement among the particle; this can be caused by the long chain of polyethylene oxide on the surface of the NCC. Based on Fig. 1, we can say that the best interaction occurred from cationic surfactant and NCC. While the modification of Tween 20 is more likely into the hydrophilic and hydrophilic relations between the polyethylene oxide and hydroxyl groups, and the modification of NCC by SDS occurred through the interaction of amphiphilic molecules and NCC.

To obtain a good understanding on the interaction between the surfactant and NCC, zeta potential measurement was conducted to get the surface charge of each modified particles. As shown in Table 1, unmodified NCC has a negative surface charge -25.24 ± 1.28 mV with a diameter of 176.1 ± 0.92 . The modification of NCC using CTAB resulted in more positive surface charge -10.39 ± 1.02 mV, a slight increase of diameter also observed 201.4 ± 10.25 nm. This phenomenon confirmed the interaction of CTAB head molecules and sulfonate ions of NCC surface. Increasing particle size also observed for SDS and Tween 20 modified NCC, which are 195 ± 7.11 and 531.6 ± 15.39 nm, respectively. It should be noted, the particle size distribution by dynamic light

Table 1
Surface charge and particle size analysis of original and modified NCC.

Material	Zeta Potential (mV)	Diameter (nm)
NCC	-25.24 ± 1.28	176.1 ± 0.92
CTAB@NCC	-10.39 ± 1.02	201.4 ± 10.25
SDS@NCC	-37.92 ± 2.11	195 ± 7.11
Tween20@NCC	-16.31 ± 0.27	531.6 ± 15.39

scattering is a system of object size interaction toward the surrounding, which is an aqueous solution. Zeta PALS regards this number as diameter since the spherical shape is assumed, meanwhile NCC has rod needle-like shaped. The zeta potential results show decreasing surface charge for SDS modified NCC and higher surface charge for nonionic modified nanoparticle, -37.92 ± 2.11 and -16.31 ± 0.27 mV, respectively. SDS is one kind of anionic surfactants; this is the reason why surface charge decreased after the modification using SDS. As for Tween 20 modified NCC, there is an increased surface charge, due to the effect of hydrogen bonding between the big head of polyethylene oxide and the hydroxyl group of NCC. Increasing particle size after the addition of surfactant was occurred due to the adsorption of surfactant onto nanoparticle, which proves that there is attractive van der Waals force occurred during the process [20,21].

The crystallinity of NCC was shown in Fig. 2, where it has a high crystalline peak at $2\theta = 22.9^\circ$ (200) and the amorphous peak around $2\theta = 16.8^\circ$ (110). Thus, the crystallinity index can be calculated using the Segal equation as follow:

$$\text{CrI (\%)} = \frac{I_{200} - I_{am}}{I_{200}} 100\% \quad (5)$$

where I_{200} and I_{am} are the intensity at crystal plane 2 0 0 and 1 1 0, respectively. From that equation, the CrI obtained is 64.31%. The surfactant-modified NCC does not show significant change at all with the diffractions peaks, because surfactant is not a crystalline matter. This can prove that surfactant will not change the physical properties of the NCC.

FTIR spectra of original and modified NCC were given in Fig. 3; there is no significant change in the spectra before and after modification with the surfactant. In fact, CTAB, SDS, and Tween 20 give similar spectra with the original NCC. Specific spectra from NCC are C—O/C—C stretching, C—H bonding, —OH bending, C—H stretching, and stretching hydroxyl group at the wavenumber of 1050, 1340, 1630, 2890, and 3300 cm^{-1} , respectively [1,2]. A little shifting was observed for CTAB modified NCC at 1357 cm^{-1} correspond to the —CH₂ wagging from the alkyl chain [22].

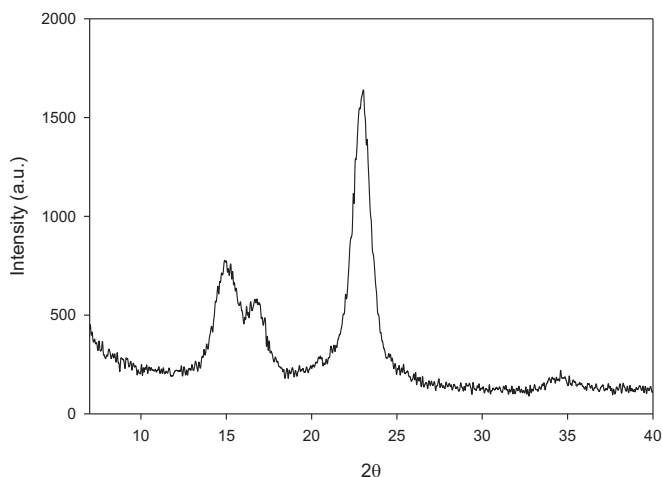


Fig. 2. XRD pattern of NCC.

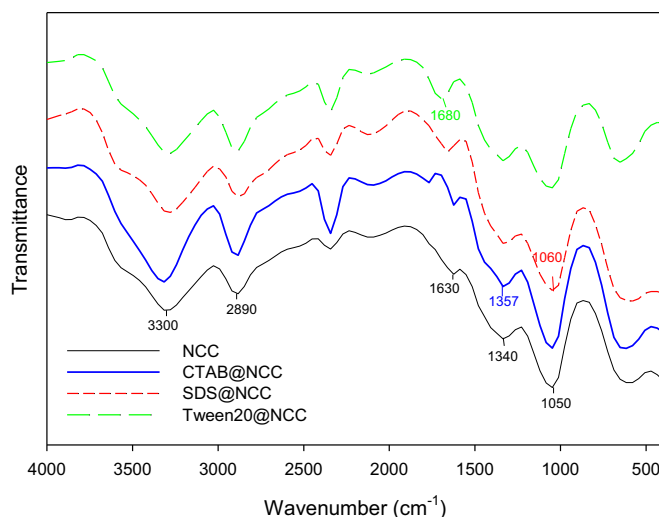


Fig. 3. FTIR spectra of original and modified NCC.

Meanwhile for SDS modified there is shifting at spectra 1060 cm^{-1} which identified as the interaction between the head of SDS and NCC [22]. There is a slight change in Tween 20 modified NCC at wavenumber 1680 cm^{-1} for the carbonyl group from the linkage of the hydrophobic and hydrophilic group of Tween 20 [23]. For the rest of the peaks, there is no alteration of the NCC chemical structure.

3.2. Drug loading

The variation concentration of surfactants with and without sodium chloride was investigated in this research. It was interesting to know that there is a significant change from ionic and nonionic surfactant based on their capacity to bind paclitaxel in the system. CTAB-NCC with salt has the best performance to bind paclitaxel with LC of 65.49 mg/g and LE 87.32%. Positive charge from the trimethyl ammonium head of CTAB forms electrostatic interaction with sulfonate group of NCC, which make it the highest drug binding. With the addition of 10 mM NaCl, there is an obvious change in the surface chemistry of NCC. There is 43% increase in loading content of paclitaxel from 45.79 to 65.49 mg/g, which means there is more surfactant attached to the NCC surface. Loading efficiency also getting stabilized with high CTAB concentration plus salt, while no addition of salt the loading efficiency decrease with higher paclitaxel concentration in the system (see Fig. 4).

Anionic surfactant tends to have lower loading content and efficiency than positively charged surfactant, and the performance is better without salt. SDS has the highest critical micelle concentration (CMC) in this study, and it has a negative head after sodium ion detached from the sulfonate ester group. CMC value of SDS is around 10 mM, lower than CMC, it is in the monomer form of surfactant molecules. Astonishingly, with 3 times increasing from 5 mM SDS does not boost the adsorption of paclitaxel toward NCC. However, the addition of salt is decreasing the PTX binding capacity, which is surprising in this case since salt lowers the CMC value and reducing the repulsion forces among the head of SDS. The highest concentration of SDS gives the highest loading content of 43.61 mg/g with the efficiency of 59.60%, with the increasing initial concentration, the loading efficiency also starts decreasing little by little due to limited adsorption area from the NCC. The difference of LC and LE is also not big, which makes it strange since it is contradictory to the original hypothesis of the hydrophilic head of surfactant interaction on hydrophilic —OH group of NCC surface.

Nonionic surfactant has the lowest loading content compared to charged surfactants, with the addition of salt 28.67 mg/g with the efficiency of 57.33%. Having lower CMC is necessary for the application of

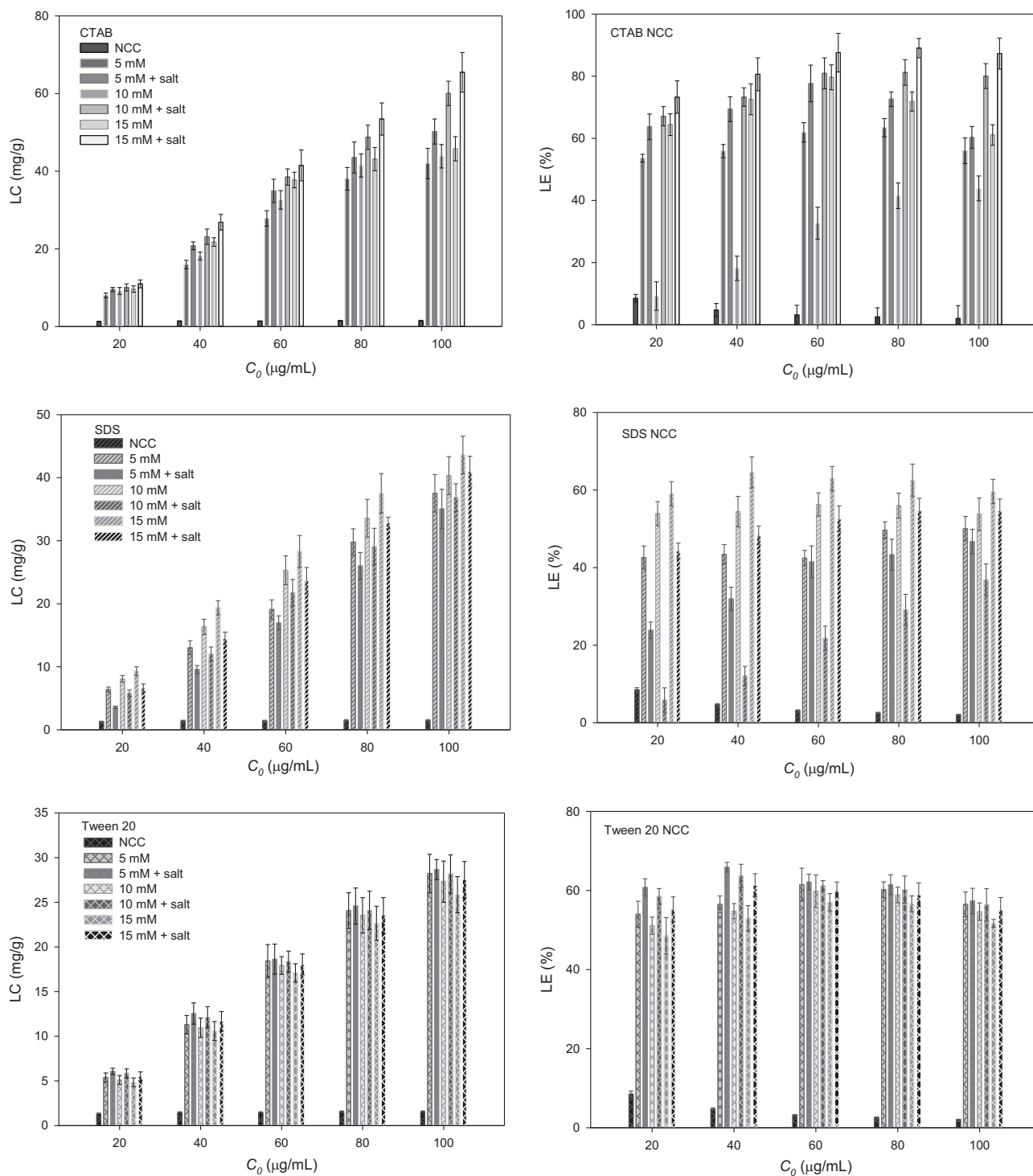


Fig. 4. PTX loading on CTAB, SDS, and Tween 20 nanocrystalline cellulose.

the drug delivery system since the micelles will stabilize the pharmaceutically active agent inside the human body while delivering toward the cancer site. It is surprising that with a high concentration of Tween 20, loading content does not show big differences in term of drug binding, but it shows a slight increase in the loading efficiency at low drug initial concentration (20 and 40 $\mu\text{g/mL}$) with the addition of 10 mM salt. Different results from CTAB and SDS is that the modification of NCC with Tween 20 plus salt managed to stabilize the drug efficiency through all of the drug concentrations. With and without adding salt in the drug loading, it does not give notable improvement for drug binding capacity. The same tendency is also observed for the increasing

surfactant concentration; it even started decreasing the loading content and efficiency slowly.

Cationic, anionic, and nonionic surfactants modified NCC have their characteristics in the drug loading system. The best performance for paclitaxel loading was obtained by the modification of NCC using CTAB with the addition of salt, following from behind is SDS with no salt, and last is Tween 20 plus salt. It was expected that CTAB@NCC has the best drug loading capacity, due to attractive forces between CTAB and NCC. Moreover, the addition of salt can even enhance the loading capacity of paclitaxel from 45.79 mg/g to 65.49 mg/g for 15 mM of CTAB. It was believed that there is the formation of second

shielding by salt ion surrounding the nanoparticle and bilayer of CTAB micelles on the surfaces of NCC. The addition of salt is actually to reduce the repulsive forces among the head of the surfactant, but it does not work for SDS. Based on Fig. 4, salt even slightly decreases the paclitaxel loading toward the modified NCC, but it manages to increase drug efficiency gradually. This effect was due to the act of sodium ion as a bridge between NCC and SDS molecules, while salt will decrease the CMC value of surfactant which forms the repetition of micelles on the surfaces NCC. Hence, salt is actually creating hydrophilic-hydrophobic interaction of the NCC and SDS. For nonionic Tween 20, it has the lowest CMC value of 0.05 mM. Tween 20 has a longer molecular structure than CTAB and SDS, because it consists of 20 polyethylene glycol unit as hydrophilic head and lauric acid as a lipophilic tail. Increasing surfactant concentration does not boost the loading capacity of paclitaxel, though adding salt intensify drug loading with minor enhancement. From these results, it can be decided that using a high concentration of Tween 20 during the modification of NCC is meaningless for the attachment of paclitaxel. Whereas the addition of salt acts as charge neutralizer for NCC who has a negative surface charge, and sodium salt can also promote more favorable interaction among the polar head of polyethylene glycol. Based on the phenomena described above, the adsorption mechanisms of PTX onto surfactant-modified NCC are mainly due to the electrostatic and van der Waals interaction between the surface of the adsorbents and PTX.

3.3. Drug release

The release kinetics of surfactant-modified NCC was studied to understand the mechanism of paclitaxel released in pH 7.4 and 5.8. Experimental data was plotted using simplified Higuchi model. Original Higuchi equation is mathematically expressed as follows:

$$\frac{M_t}{M_\infty} = \sqrt{DC_s(2A - C_s)t} \quad (6)$$

where $\frac{M_t}{M_\infty}$ is the cumulative drug release, D is the diffusivity of the drug, A is the total amount of drug in the carrier, and C_s is the solubility of the drug in the matrix substance. To make the calculation easier, Eq. (6) can be simplified as

$$\frac{M_t}{M_\infty} = k_H t^{\frac{1}{2}} \quad (7)$$

Simplified Higuchi Eq. (7) has a parameter k_H as the complex Higuchi constant, which is further used in this study for the fitting model of experimental data. Higuchi equation can be used to describe the sustained release behavior of the drug through the solution based on a pseudo-steady state approach of Fick's second law of diffusion. The plotted model was shown in Fig. 5, which was not fitted well toward the experimental data of CTAB@NCC.

Noticing that the experimental data has S-shape, we try to plot using the Sigmoidal function on it. There are several sigmoidal functions available, the function that is chosen in this study is the original Sigmoidal three parameters function. Some researchers studied drug release reported that they have sigmoidal shape release data, but only a few researchers mention about fitting experimental data using a sigmoidal model [24–29]. The most common drug release model used to describe a sigmoidal curve is the Weibull model. However, it cannot fit with the experimental data in this study [30]. Duvvuri and co-authors make a modification of the sigmoidal equation which consists of 5 parameters to describe the phase I and phase II of drug release [31]. The sigmoidal function used in this study has the following form

$$\frac{M_t}{M_\infty} = \frac{R_{\max}}{1 + e^{-k(t-t_{50})}} \quad (8)$$

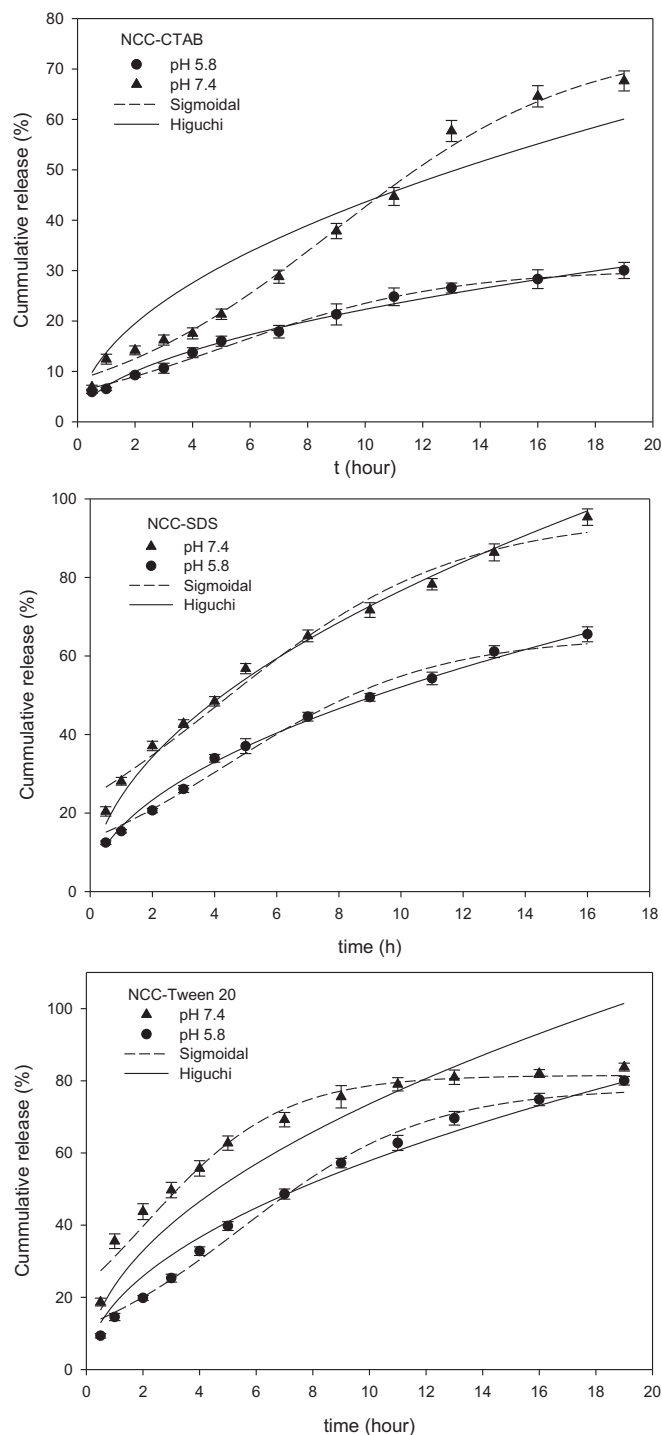


Fig. 5. Drug release profile of modified NCC at pH 5.8 and 7.4.

where R_{\max} is the theoretical maximum release, k indicates the release rate (h^{-1}), and t_{50} is the time required to obtain 50% of maximum drug release (h). As shown in Fig. 5, all modified NCC have sustained released behavior of paclitaxel at both pH condition. At phosphate buffer pH 5.8, the cumulative release is lower than pH 7.4, which means that the PTX loaded NCC is suitable for oral drug delivery. Sigmoidal can fit through all release profile in this study as can be seen in Fig. 5. However, it missed several points of experimental data at SDS modified NCC, especially at the beginning of the release point. It is amazing how Higuchi can fit almost every data in the plot, except for CTAB and Tween 20 modified NCC at simulated body fluid condition. The Higuchi equation cannot fit at those data, due to its limitation. Clear observation from both conditions is that

Higuchi failed to fit the experimental data because it has the rapid onset of drug dissolution from the solution rather than diffusion from bulk concentration to the solution. While sigmoidal function can fit through all of the experimental data very well since it has the theoretical value of the maximum cumulative release, thus, the model can predict the maximum $\frac{M_t}{M_\infty}$ based on the real data of release and manage to give good fitting throughout all of the graphs.

All of the value of the parameter is described in Table 2; sigmoidal has a good value of sum square or error for three modified NCC at both pH condition with an R^2 value range from 0.97 until 0.99. Higuchi model cannot fit only 2 experimental data since they have not yet reached uniform concentration out of the amount of the initial drug on the CTAB and Tween 20 modified NCC for pH 7.4. Higuchi can fit SDS@NCC for both conditions since it reached almost saturation in the solution, despite the saturation assumption of Higuchi, all drug release profiles at pH 5.8 can match the Higuchi very well. One of the assumptions in the Higuchi model is the approach of constant diffusivity of the drug in the release system. Therefore, at pH 5.8, the drug release rate was constant and linear cumulative release with continuous time. Judging from the sigmoidal fitting, it seems that the function is very flexible at different kind of release profile than the Higuchi model. Paul and McSpadden gave a wonderful elaboration toward the Higuchi equation using Fick's second law; they discussed the condition to achieve results based on exact analysis of drug release through the partial differential equation based on distance and time [32]. Later they obtained erf result which approach unity for special cases, mathematically erf is a special case of sigmoidal shape occurs in partial differential equations to describe diffusion. Rather than using erf in this fitting model, we use the empirical equation of sigmoidal 3 parameters function, and it gives good fitting for all experimental data in this study.

By changing the pH of the system, the surface charge of surfactant-modified NCCs also changed, and the amount of drug release to the solution also changed. With pKa value of 10.36, the electrostatic interaction between PTX and hydroxyl ions in the solution increased as the pH increased, and the amount of PTX released to the solution also increased, and this phenomenon confirms that the electrostatic interaction played the significant role during uptake and release of PTX.

3.4. *In vitro* cell cytotoxicity

Cell viability was determined to check the biocompatibility of the materials toward mouse osteoblast cells 7F2 using MTT assay.

Table 2
Higuchi and sigmoidal fitting parameters of kinetic release.

Modified NCC	Parameters	pH 5.8	pH 7.4
CTAB	Higuchi		
	k_H	7.0556	13.7855
	R^2	0.9891	0.8882
	Sigmoidal		
	R_{max} (%)	30.1896	75.5441
	k (h^{-1})	0.2641	0.2346
	t_{50} (h)	5.2394	8.8836
SDS	Higuchi		
	k_H	16.4789	24.2393
	R^2	0.994	0.9914
	Sigmoidal		
	R_{max} (%)	65.0329	95.5241
	k (h^{-1})	0.3036	0.263
	t_{50} (h)	4.4392	4.128
Tween 20	Higuchi		
	k_H	18.2901	23.2711
	R^2	0.9779	0.774
	Sigmoidal		
	R_{max} (%)	78.0532	81.5184
	k (h^{-1})	0.3063	0.4207
	t_{50} (h)	5.4627	2.125
	R^2	0.9901	0.9732

NCC does not show any toxic behavior toward the cells line 7F2; increasing NCC concentration even increases the cells viability in the medium. It was observed that using CTAB as modifier was not compatible at all since around 80% of cells died at 10 $\mu\text{g}/\text{mL}$ of particle suspension. Anionic surfactant was less toxic than CTAB, but with the increasing particle in the medium suspension fewer cells survived in the media (around 50%). This might be happened due to cytolytic activity from SDS that leads to cells damage [33]. From Fig. 6, we can see that the modification of Tween 20 can sustain 64% viable cells at 100 $\mu\text{g}/\text{mL}$ NCC suspension, which proves that nonionic is the best in terms of interaction between surfactant molecules and cells.

The surfactant was known to be quite toxic for cells because it can promote lysis at the cells membrane. The especially cationic surfactant was highly toxic due to its anticholinergic activity of monoquarternary ammonium salts; thus it was not suggested for CTAB to be administered intravenously. However, *in vivo* studies regarding CTAB *via* oral route in the rat was located in the gastrointestinal tract 8 h after administration and it was excreted in the feces and urine around 93% after 3 days [34]. Nonionic surfactant like Tween 20 which consists of lauric acid joined with polyethylene glycol by ester linkage was split by intestinal lipase, and polyethylene glycol is not well absorbed in the body, this was found in feces. While a small amount which is absorbed, is excreted in the urine. Anionic alkyl sulfates surfactant is rapidly absorbed from the GI-tract and excreted in the urine of rats. The human body is more complex than cells, and the high toxicity from *in vitro* study was not completely able to become a reference that surfactant itself is hazardous for human consumption.

4. Conclusion

CTAB modified nanocrystalline cellulose has the best performance in terms of loading and release of paclitaxel at pH 5.8 and 7.4. SDS modified nanocrystalline cellulose has the lowest loading of paclitaxel which is 43.61 mg/g, with the highest cumulative release of 95% at pH 7.4 and 65% at pH 5.8 for 16 h. Tween 20 modified nanocrystalline cellulose can sustain the release until 19 h for around 80% at pH 5.8 and 7.4. Higuchi model cannot fit through all of the experimental data, while a sigmoidal function was able to fit the data due to its flexibility through all release rate. Cytotoxicity assay of modified nanoparticle give low cell viability with the increasing nanocrystalline cellulose in the suspension, it is not suggested for intravenous route due to high apoptosis from all of the surfactants.

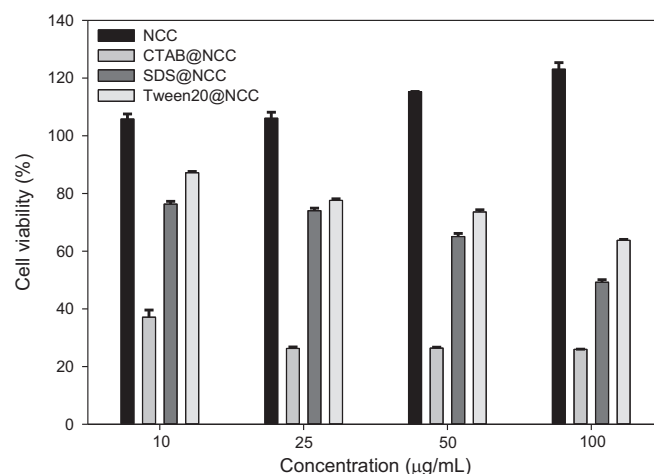


Fig. 6. Cell viability of 7F2 cells after treatment with modified and normal NCC.

References

- [1] N. Zainuddin, I. Ahmad, H. Kargarzadeh, S. Ramli, Hydrophobic kenaf nanocrystalline cellulose for the binding of curcumin, *Carbohydr. Polym.* 163 (2017) 261–269, <https://doi.org/10.1016/j.carbpol.2017.01.036>.
- [2] W. Qing, Y. Wang, Y. Wang, D. Zhao, X. Liu, J. Zhu, The modified nanocrystalline cellulose for hydrophobic drug delivery, *Appl. Surf. Sci.* 366 (2016) 404–409, <https://doi.org/10.1016/j.apsusc.2016.01.133>.
- [3] J.K. Jackson, K. Letchford, B.Z. Wasserman, L. Ye, W.Y. Hamad, H.M. Burt, The use of nanocrystalline cellulose for the binding and controlled release of drugs, *Int. J. Nanomedicine* 6 (2011) 321–330, <https://doi.org/10.2147/IJN.S16749>.
- [4] V. Mohanta, G. Madras, S. Patil, Layer-by-layer assembled thin films and microcapsules of nanocrystalline cellulose for hydrophobic drug delivery, *ACS Appl. Mater. Interfaces* 6 (2014) 20093–20101, <https://doi.org/10.1021/am405633r>.
- [5] M.T. Huizing, V.H.S. Misser, R.C. Pieters, W.W. ten Bokkel Huinink, C.H.N. Veenhof, J.B. Vermorken, H.M. Pinedo, J.H. Beijnen, Taxanes: a new class of antitumor agents, *Cancer Invest.* 13 (1995) 381–404, <https://doi.org/10.3109/07357909509031919>.
- [6] B.A. Weaver, How taxol/paclitaxel kills cancer cells, *Mol. Biol. Cell* 25 (2014) 2677–2681, <https://doi.org/10.1091/mbc.E14-04-0916>.
- [7] M. Narvekar, H.Y. Xue, J.Y. Eoh, H.L. Wong, Nanocarrier for poorly water-soluble anticancer drugs—barriers of translation and solutions, *AAPS PharmSciTech* 15 (2014) 822–833, <https://doi.org/10.1208/s12249-014-0107-x>.
- [8] M.S. Surapaneni, S.K. Das, N.G. Das, Designing paclitaxel drug delivery systems aimed at improved patient outcomes: current status and challenges, *ISRN Pharmacol.* 2012 (2012) 1–15, <https://doi.org/10.5402/2012/623139>.
- [9] H. Gelderblom, J. Verweij, K. Nooter, A. Sparreboom, E.L. Cremophor, The drawbacks and advantages of vehicle selection for drug formulation, *Eur. J. Cancer* 37 (2001) 1590–1598, [https://doi.org/10.1016/S0959-8049\(01\)00171-X](https://doi.org/10.1016/S0959-8049(01)00171-X).
- [10] O.C. Farokhzad, R. Langer, Impact of nanotechnology on drug delivery, *ACS Nano* 3 (2009) 16–20, <https://doi.org/10.1021/nn900002m>.
- [11] K.B. Sutradhar, M.L. Amin, Nanotechnology in cancer drug delivery and selective targeting, *ISRN Nanotechnol.* 2014 (2014) 1–12, <https://doi.org/10.1155/2014/939378>.
- [12] W.H. De Jong, P.J. a Borm, Drug delivery and nanoparticles: applications and hazards, *Int. J. Nanomedicine* 3 (2008) 133–149, <https://doi.org/10.2147/IJN.S596>.
- [13] C. Wang, H. Huang, M. Jia, S. Jin, W. Zhao, R. Cha, Formulation and evaluation of nanocrystalline cellulose as a potential disintegrant, *Carbohydr. Polym.* 130 (2015) 275–279, <https://doi.org/10.1016/j.carbpol.2015.05.007>.
- [14] Y. Zhang, Q. Zhao, H. Wang, X. Jiang, R. Cha, Preparation of green and gelatin-free nanocrystalline cellulose capsules, *Carbohydr. Polym.* 164 (2017) 358–363, <https://doi.org/10.1016/j.carbpol.2017.01.096>.
- [15] V.P. Torchilin, Structure and design of polymeric surfactant -based drug delivery systems, *J. Control. Release* 73 (2001) 137–172.
- [16] S. Ishikawa, Y. Matsumura, K. Katoh-Kubo, T. Tsuchido, Antibacterial activity of surfactants against *Escherichia coli* cells is influenced by carbon source and anaerobiosis, *J. Appl. Microbiol.* 93 (2002) 302–309, <https://doi.org/10.1046/j.1365-2672.2002.01690.x>.
- [17] H. Kobayashi, R. Watanabe, P.L. Choyke, Improving conventional enhanced permeability and retention (EPR) effects; what is the appropriate target? *Theranostics* 4 (2014) 81–89, <https://doi.org/10.7150/thno.7193>.
- [18] E. Blanco, H. Shen, M. Ferrari, Principles of nanoparticle design for overcoming biological barriers to drug delivery, *Nat. Biotechnol.* 33 (2015) 941–951, <https://doi.org/10.1038/nbt.3330>.
- [19] P.W. Sylvester, Drug design and discovery: methods and protocols, *Methods Mol. Biol.* 2011, pp. 157–168, <https://doi.org/10.1007/978-1-61779-012-6>.
- [20] H. Yamada, C. Urata, S. Higashimori, Y. Aoyama, Y. Yamauchi, K. Kuroda, Critical roles of cationic surfactants in the preparation of colloidal mesostructured silica nanoparticles: control of mesostructure, particle size, and dispersion, *ACS Appl. Mater. Interfaces* 6 (2014) 3491–3500, <https://doi.org/10.1021/am405633r>.
- [21] L. Zhong, S. Fu, X. Peng, H. Zhan, R. Sun, Colloidal stability of negatively charged cellulose nanocrystalline in aqueous systems, *Carbohydr. Polym.* 90 (2012) 644–649, <https://doi.org/10.1016/j.carbpol.2012.05.091>.
- [22] R.B. Viana, A.B.F. Da Silva, A.S. Pimentel, Infrared spectroscopy of anionic, cationic, and zwitterionic surfactants, *Adv. Phys. Chem.* 2012 (2012) 1–15, <https://doi.org/10.1155/2012/903272>.
- [23] M.C. Ortiz-Tafoya, A. Tecante, Physicochemical characterization of sodium stearyl lactylate (SSL), polyoxyethylene sorbitan monolaurate (Tween 20) and κ -carrageenan, *Data Brief* 19 (2018) 642–650, <https://doi.org/10.1016/j.dib.2018.05.064>.
- [24] Q. Shang, A. Zhang, Z. Wu, S. Huang, R. Tian, In vitro evaluation of sustained release of risperidone-loaded microspheres fabricated from different viscosity of PLGA polymers, *Polym. Adv. Technol.* 29 (2018) 384–393, <https://doi.org/10.1002/pat.4125>.
- [25] I. Lozoya-Agullo, I. González-Álvarez, M. González-Álvarez, M. Merino-Sanjuán, M. Bermejo, In situ perfusion model in rat colon for drug absorption studies: comparison with small intestine and Caco-2 cell model, *J. Pharm. Sci.* 104 (2015) 3136–3145, <https://doi.org/10.1002/jps.24447>.
- [26] T. An, J. Choi, A. Kim, J.H. Lee, Y. Nam, J. Park, B.K. Sun, H. Suh, C.J. Kim, S.J. Hwang, Sustained release of risperidone from biodegradable microspheres prepared by in-situ suspension-evaporation process, *Int. J. Pharm.* 503 (2016) 8–15, <https://doi.org/10.1016/j.ijpharm.2016.02.023>.
- [27] W. Chen, A. Palazzo, W.E. Hennink, R.J. Kok, Effect of particle size on drug loading and release kinetics of gefitinib-loaded PLGA microspheres, *Mol. Pharm.* 14 (2017) 459–467, <https://doi.org/10.1021/acs.molpharmaceut.6b00896>.
- [28] H. Tu, Y. Qu, X. Hu, Y. Yin, H. Zheng, P. Xu, F. Xiong, Study of the sigmoidal swelling kinetics of carboxymethylchitosan-g-poly(acrylic acid) hydrogels intended for colon-specific drug delivery, *Carbohydr. Polym.* 82 (2010) 440–445, <https://doi.org/10.1016/j.carbpol.2010.04.086>.
- [29] T. Nakajima, I. Takeuchi, H. Ohshima, H. Terada, K. Makino, Push-pull controlled drug release systems: effect of molecular weight of polyethylene oxide on drug release, *J. Pharm. Sci.* 107 (2018) 1896–1902, <https://doi.org/10.1016/j.xphs.2018.02.022>.
- [30] F. Langenbucher, Letters to the editor: linearization of dissolution rate curves by the Weibull distribution, *J. Pharm. Pharmacol.* 24 (1972) 979–981, <https://doi.org/10.1111/j.2042-7158.1972.tb08930.x>.
- [31] S. Duvvuri, K. Gaurav Janoria, A.K. Mitra, Effect of polymer blending on the release of ganciclovir from PLGA microspheres, *Pharm. Res.* 23 (2006) 215–223, <https://doi.org/10.1007/s11095-005-9042-6>.
- [32] D.R. Paul, S.K. McSpadden, Diffusional release of a solute from a polymer matrix, *J. Membr. Sci.* 1 (1976) 33–48, [https://doi.org/10.1016/S0376-7388\(00\)82256-5](https://doi.org/10.1016/S0376-7388(00)82256-5).
- [33] F.G. Bartnik, Interaction of anionic surfactants with protein, enzymes, and membranes, in: C. Gloxhuber, K. Kunstler (Eds.), *Anionic Surfactants Biochem. Toxicol. Dermatology*, 2nd ed. Marcel Dekker, Inc., United States of America 1992, pp. 1–42.
- [34] D. Attwood, A.T. Florence, *Surfactant Systems: Their Chemistry, Pharmacy and Biology*, Chapman and Hall, New York, 1983.